Reflection Model and High-Energy $\pi^- p$ Backward Peaks

MING CHIANG LI
Department of Physics, Virginia Polytechnic Institute, Blacksburg, Virginia 24061
(Received 21 April 1969)

We propose a classical optical model for high-energy elastic scattering. The model predicts that the logarithmic slopes for forward differential cross sections should be either the same or twice as large as the backward ones. The backward peak is due to the contribution from the discontinuity in the boundary of the optical medium. The model has the property that the mechanisms responsible for the forward and backward scatterings are not independent of each other. This is contrasted with conventional models which view the forward and backward scatterings as arising from independent mechanisms. For example, in absorptive and Regge-pole models the main contribution to the forward scattering comes from t-channel exchange, while backward scattering arises from u-channel exchange. A fit is made to the high-energy $\pi^- p$ data in both forward and backward directions, and good results are obtained.

INTRODUCTION

EXPERIMENTS on elastic high-energy scattering generally exhibit the following characteristics: (a) a forward diffraction peak, (b) a backward peak, (c) a differential cross section which approaches a limit as the incoming energy $\rightarrow \infty$:

$$\lim \frac{d\sigma}{dt} = f(t).$$

It should be noted that similar characteristics are also observed in classical scattering. The forward peak in high-energy scattering is called a diffraction peak because of its presumed similarity to the diffraction patterns in classical electrodynamics. However, these two scattering phenomena are qualitatively different. In the diffraction and scattering problems of classical electrodynamics, the diffraction peak, or backward peak, is flatter than the corresponding one in high-energy scattering. In the classical case the scattering targets are the geometric apertures or obstacles. These targets have a clear and distinct boundary which gives rise to the "flatness" of both peaks in classical scattering. In the geometrical-optics limit for classical scattering, the forward scattering amplitude is analogous to the transmission amplitude for an electromagnetic wave through a medium, and the backward amplitude is analogous to the reflected one. For a given scattering the geometrical-optics limit is a high-frequency or short-wavelength limit. If there is a similarity between high-energy and classical scatterings, one can conjecture that the forward and backward peaks observed in the high-energy scattering also come from some sort of transmission and reflection mechanisms. In this paper we propose such a mechanism.

A convenient way to explore this classical feature is to treat the high-energy scattering as a potential problem. However, the potential being "strong," the problem generally can not be solved exactly, and some approximate methods must be used. The most commonly used methods are the so-called WKB method and its linear approximation, the eikonal approximation.[1] These approximations are only valid for the forward scattering and are based on an assumption that the scattering potential changes very slowly over a distance comparable to the incident wavelength $1/k$. Any rapid change in the potential, which might be the case in high-energy scattering, will cause a reflection or a backward scattering. These approximation methods serve a purpose in understanding the classical features of the high-energy scattering, but should not be considered as complete since they cannot describe the backward scattering. Therefore, we will not use the WKB method or its linear approximations, but instead we use a simple solvable model which enables us to calculate both the forward and backward amplitude.

The model we will consider has the property that the mechanisms responsible for the forward and backward scatterings are not totally independent. This is not the case in the most conventional treatment of the high-energy scattering. In most common treatments, the main contribution to backward scattering comes from the exchange potential,[2] i.e., the so-called Majorana force. This force gives a constructive interference between even- and odd-parity states. The interference leads to an accumulative contribution in the backward direction. On the other hand, the forward amplitude comes from the ordinary potential. Thus the amplitudes in forward and backward directions are from two distinctly different mechanisms. In the absorptive[3] and Regge-pole[4] models, both forward and backward scattering amplitudes are due to t-channel and u-channel exchanges, respectively, which are also different from each other. In the classical case the transmission and reflection waves occur simultaneously as a wave passes through one medium and into the other. The appear-

[1] G. Wentzel, Z. Physik **38**, 518 (1926); H. A. Kramers, *ibid.* **39**, 828 (1926); M. Brillouin, J. Phys. **3**, 65 (1922).

[2] J. M. Blatt and V. F. Weisskopf, *Theoretical Nuclear Physics* (John Wiley & Sons, Inc., New York, 1952).

[3] K. Gottfried and J. D. Jackson, Nuovo Cimento **34**, 735 (1964); J. D. Jackson, Rev. Mod. Phys. **37**, 484 (1965); L. Durand and Y. T. Chiu, Phys. Rev. Letters **12**, 399 (1964); **13**, 45(E) (1964).

[4] V. Barger and D. Cline, Phys. Rev. **155**, 1792 (1967); **21**, 392 (1968); and (unpublished).

ance of these two waves is due to a discontinuity on the boundary. Although the generating mechanisms may be different for both waves, they are not totally independent.

In this paper we shall consider scattering of two spinless particles. For particles with spin, there would be a spin-flip and a non-spin-flip amplitude. The spin-flip amplitude gives a small contribution in both forward and backward directions. It is customary to assume that, as long as one is only interested in the non-spin-flip amplitude, the spin need not be taken into consideration. With the above considerations we might expect our model to be applicable to high-energy scattering in both forward and backward directions.

The presentation is arranged in the following order. In Sec. 1 we list the results for scattering by a square-well potential in the one-dimensional case. This one-dimensional problem may be considered as the problem of a plane wave incident normally on a well, which is confined by two parallel infinite planes. In Sec. 2 we discuss the scattering by a square well in the three-dimensional case. The forward and backward amplitudes are expressly factored out to show that, in the high-energy limit, they exhibit the same property as do the transmitted and reflected wave amplitudes in Sec. 1. The model here is essentially an optical model, in which the potential is considered as a description of the optical medium. Owing to Lorentz contraction, the shape of most objects is pancakelike at high energy. Our intuition indicates that it may be reasonable to consider a disk-shaped well, rather than the square well for a comparison with experiments. This approach is described in Sec. 3. In Sec. 4 we present a comparison between the theory of Sec. 3 and $\pi^- p$ experimental data at several incident energies. Our model is a single-energy model for both the forward and backward scatterings. The reported data are given at different incident energies. We choose data for two neighboring incident energies from one of each forward and backward direction as a fitting unit. The numerical values show that the fits are good. Our model may provide valuable clues as to the nature of high-energy scattering.

1. TRANSMISSION AND REFLECTION

Let us now consider a plane wave incident normal to a rectangular well which is confined by two parallel infinite planes. The potential in the well will be taken as complex throughout this paper. The imaginary part of the potential describes the summation of inelastic processes. The problem described in this section is one-dimensional and can be found in most textbooks on quantum mechanics.[5] The ratio of the transmitted and incident wave amplitudes can be written as

$$T=\frac{2ikk'e^{-2ika}}{(k^2+k'^2)\sin(2k'a)+2ikk'\cos(2k'a)}, \quad (1.1)$$

where

$$k=(2mE)^{1/2},$$
$$k'=[2m(E-V)]^{1/2}. \quad (1.2)$$

The energy and mass of the incident particle are denoted by E and m. The well has a complex potential V and a range $2a$. The ratio of the reflected and incident wave amplitudes is given by

$$R=\frac{(k^2-k'^2)\sin(2k'a)e^{-2ika}}{(k^2+k'^2)\sin(2k'a)+2ikk'\cos(2k'a)}. \quad (1.3)$$

The transmitted and reflected waves include not only the contribution from the primary transmission and reflection, but also from internal and secondary reflections at the boundaries. If the potential is strongly absorptive, the contributions from secondary reflections can be neglected. Then

$$T\approx[4kk'/(k+k')^2]e^{2i(k'-k)a}, \quad (1.4)$$

$$R\approx[(k-k')/(k+k')]e^{-2ika}. \quad (1.5)$$

Equation (2.5) expresses the fact that the reflected wave depends on the wave-number discontinuity $k-k'$, which takes place on the boundary. On the other hand, Eq. (1.4) indicates that the transmitted wave is just the incident wave, modified by losses due to absorption inside the potential and by reflections on the boundaries.

2. SQUARE-WELL SCATTERING

For a square-well potential, the scattering problem can be solved exactly. The formula discussed here will serve as a foundation for our later discussion. The complex square well is confined within radius a:

$$V(r)=V', \quad r<a$$
$$=0, \quad r>a \quad (2.1)$$

where $V'=V_1'+iV_2'$. The radical function $u_{l,k}(r)$ for each partial wave satisfies the Schrödinger equation

$$\left(-\frac{d^2}{dr^2}+\frac{l(l+1)}{r^2}-k^2\right)u_{l,k}(r)=0, \quad r>a$$
$$\left(-\frac{d^2}{dr^2}+\frac{l(l+1)}{r^2}-k'^2\right)u_{l,k}(r)=0, \quad r<a \quad (2.2)$$

where $k'^2=k^2-2\mu V'$, μ is the reduced mass, and k is the incident momentum. The phase shift δ_l for each partial wave satisfies the following relation:

$$e^{i\delta_l}\sin\delta_l=\frac{1}{2i}(e^{2i\delta_l}-1)$$
$$=e^{2i\epsilon_l}\left(\frac{S_l}{\beta_l-\Delta_l-iS_l}+e^{-i\epsilon_l}\sin\epsilon_l\right). \quad (2.3)$$

[5] For example, E. Merzbacher, *Quantum Mechanics* (John Wiley & Sons, Inc., New York, 1961).

The parameters ϵ_l, S_l, β_l, and Δ_l are determined by

$$\Delta_l+iS_l=ka\frac{j_l'(ka)+in_l'(ka)}{j_l(ka)+in_l(ka)},$$
$$\beta_l=k'a\frac{j_l'(k'a)}{j_l(k'a)}, \tag{2.4}$$
$$e^{2i\epsilon_l}=-\frac{j_l(ka)-in_l(ka)}{j_l(ka)+in_l(ka)},$$

where j_l and n_l are spherical Bessel functions. The differential cross section in terms of phase shift has the form

$$\frac{d\sigma}{d\Omega}=\frac{1}{k^2}\left|\sum_{l=0}^{\infty}(2l+1)e^{i\delta_l}\sin\delta_l P_l(\cos\theta)\right|^2, \tag{2.5}$$

where θ is the scattering angle in the center-of-mass frame. We wish to explore the behavior of the forward and backward scatterings in the above model. The scattering amplitudes for these two types can have simple approximate forms with high accuracy. Some important physical quantities such as momenta u and t and impact parameter b should be introduced:

$$-t=2k^2(1-\cos\theta), \quad -u=2k^2(1+\cos\theta), \tag{2.6}$$
$$bk=l+\tfrac{1}{2}. \tag{2.7}$$

In the forward direction, θ is always small; therefore, t momentum may be approximated by

$$-t\approx 2k^2(1-1+\tfrac{1}{2}\theta^2)=k^2\theta^2. \tag{2.8}$$

Meanwhile the Legendre function $P_l(\cos\theta)$ at such small angles can be represented by a zeroth-order Bessel function $J_0[\theta(l+\frac{1}{2})]$:

$$P_l(\cos\theta)\approx J_0[\theta(l+\tfrac{1}{2})]=J_0(b\sqrt{-t}), \quad \text{for } \theta \text{ small}. \tag{2.9}$$

Let

$$e^{i\delta_l}\sin\delta_l\equiv\alpha_l\equiv\alpha(b); \tag{2.10}$$

then the differential cross section in forward direction has the form

$$\frac{d\sigma}{dt}=4\pi\left|\int\alpha(b)J_0(b\sqrt{-t})bdb\right|^2. \tag{2.11}$$

In backward direction, θ is close to π; the defined angle $\theta'=\pi-\theta$ should be small. The momentum u can be written as

$$-u=2k^2(1-\cos\theta')\approx k^2\theta'^2. \tag{2.12}$$

The Legendre function $P_l(\cos\theta)$ for backward scattering angles may also be approximately expressed by a zeroth-order Bessel function

$$P_l(\cos\theta)=P_l(-\cos\theta')=(-)^lP_l(\cos\theta'),$$
$$e^{il\pi}J_0[\theta'(l+\tfrac{1}{2})]=e^{i(bk-1/2)\pi}J_0(b\sqrt{-u}). \tag{2.13}$$

The corresponding differential cross section in backward direction is given by

$$\frac{d\sigma}{du}=4\pi\left|\int\alpha(b)e^{i(kb-1/2)\pi}J_0(b\sqrt{-u})bdb\right|^2. \tag{2.14}$$

The differential cross sections in Eqs. (2.11) and (2.14) behave differently. The forward cross section comes mainly from the smooth part in the odd and even partial-wave amplitudes α_l. On the other hand, the backward cross section comes from the nonsmooth part. This latter part can be easily produced by an exchange mechanism, for example, the Majorana exchange potential, or the u-channel exchange. In the square-well model, there is no exchange mechanism involved. It is our intention to seek out what contributes most to the backward cross section in this simple naive model. One must bear in mind that in high-energy scattering, the number of partial-wave amplitudes involved is quite high. Hence, we limit ourselves only to the case $ka\gg1$. In order not to complicate the problem, $|k'|$ is treated in the same order as k. It is known that the forms of the asymptotic expansions for the Bessel functions depend on their orders and arguments.[6] The partial-wave amplitude is best discussed by dividing them in different regions which are denoted by $l\ll ka$, $l<ka$, $l\sim ka$, and $l>ka$. These regions are denoted by A, B, C, and D, respectively. The reason for which we divide the orbital momentum in several regions is due to the validity of the asymptotic forms of the Bessel functions. Each region overlaps with its adjacent ones; however, it is convenient to treat each of these as separate regions. In the following, the relevant quantities are given in the corresponding group along with the asymptotic expansions which are used to calculate them.

Region A. $l\ll ka$, $ka\gg1$.

Asymptotic expansions:

$$\begin{aligned} j_l(ka)&\approx\cos[ka-\tfrac{1}{2}(l+1)\pi]/ka,\\ n_l(ka)&\approx\sin[ka-\tfrac{1}{2}(l+1)\pi]/ka,\\ j_l'(ka)&\approx-\sin[ka-\tfrac{1}{2}(l+1)\pi]/ka,\\ n_l'(ka)&\approx\cos[ka-\tfrac{1}{2}(l+1)\pi]/ka. \end{aligned} \tag{2.15}$$

Relevant quantities:

$$\begin{aligned} &e^{2i\epsilon_l}\approx(-)^le^{-2ika},\\ &\Delta_l+iS_l\approx ika,\\ &\beta_l\approx k'a\cot k'a, \quad l=\text{even}\\ &\quad\approx-k'a\tan k'a, \quad l=\text{odd},\\ &e^{2i\delta_l}\approx\frac{k'\cot k'a+ik}{k'\cot k'a-ik}e^{-2ika}, \quad l=\text{even}\\ &\quad\approx-\frac{k'\tan k'a-ik}{k'\tan k'a+ik}e^{-2ika}, \quad l=\text{odd}. \end{aligned} \tag{2.16}$$

[6] *Higher Transcendental Functions*, edited by A. Erdélyi *et al.* (McGraw-Hill Book Co., New York, 1953); *Handbook of Mathematical Functions*, edited by M. Abramowitz and I. A. Stegun (U. S. Department of Commerce, National Bureau of Standards, Washington, D. C., 1964).

Region B. $l<ka$, $ka\gg1$.

Asymptotic expansions:

$$\begin{aligned}
j_l(ka)&\approx\frac{1}{(ka\nu\tan\beta)^{1/2}}\cos(\nu\tan\beta-\nu\beta-\tfrac{1}{4}\pi),\\
n_l(ka)&\approx\frac{1}{(ka\nu\tan\beta)^{1/2}}\sin(\nu\tan\beta-\nu\beta-\tfrac{1}{4}\pi),\\
j_l'(ka)&\approx\left(\frac{\sin2\beta}{2ka\nu}\right)^{1/2}\sin(\nu\tan\beta-\nu\beta-\tfrac{1}{4}\pi),\\
n_l'(ka)&\approx\left(\frac{\sin2\beta}{2ka\nu}\right)^{1/2}\cos(\nu\tan\beta-\nu\beta-\tfrac{1}{4}\pi),
\end{aligned}\tag{2.17}$$

where

$$\nu\equiv l+\tfrac{1}{2}=kb,\quad \nu\sec\beta\equiv ka,\quad \nu\sec\beta'\equiv k'a.\tag{2.18}$$

Relevant quantities:

$$\begin{aligned}
e^{2i\epsilon_l}&\approx-\exp[-2i(\nu\tan\beta-\nu\beta-\tfrac{1}{4}\pi)],\\
\Delta_l+iS_l&\approx ika\sin\beta,\\
\beta_l&\approx-k'a\sin\beta'\tan(\nu\tan\beta'-\nu\beta'-\tfrac{1}{4}\pi),\\
e^{2i\delta_l}&\approx\frac{1+\rho\epsilon^{-2iA'}}{1+\rho\epsilon^{2iA'}}e^{-2i(A-A')},
\end{aligned}\tag{2.19}$$

where

$$\begin{aligned}
A&\equiv\nu\tan\beta-\nu\beta-\tfrac{1}{4}\pi,\\
A'&\equiv\nu\tan\beta'-\nu\beta'-B\pi,\\
\rho&\equiv\frac{\tan\beta-\tan\beta'}{\tan\beta+\tan\beta'}\\
&=\frac{k\cos(\frac{1}{2}\pi-\beta)-k'\cos(\frac{1}{2}\pi-\beta')}{k\cos(\frac{1}{2}\pi-\beta)+k'\cos(\frac{1}{2}\pi-\beta')}.
\end{aligned}\tag{2.20}$$

ρ is the so-called Fresnel reflection coefficients; it represents the reflection of a plane wave with incident angle $\frac{1}{2}\pi-\beta$ from the boundary of a potential step, and the transmitted wave has a transmitted angle $\frac{1}{2}\pi-\beta'$.

Region C. $l\sim ka$, $ka\gg1$.

Asymptotic expansions:

$$\begin{aligned}
j_l(ka)&\approx\left(\frac{\pi}{2ka}\right)^{1/2}\frac{2^{1/3}}{\nu^{1/3}}\mathrm{Ai}(-2^{1/3}z),\\
n_l(ka)&\approx-\left(\frac{\pi}{2ka}\right)^{1/2}\frac{2^{1/3}}{\nu^{1/3}}\mathrm{Bi}(-2^{1/3}z),\\
j_l'(ka)&\approx-\left(\frac{\pi}{2ka}\right)^{1/2}\frac{2^{2/3}}{\nu^{2/3}}\mathrm{Ai}'(-2^{1/3}z),\\
n_l'(ka)&\approx\left(\frac{\pi}{2ka}\right)^{1/2}\frac{2^{2/3}}{\nu^{2/3}}\mathrm{Bi}'(-2^{1/3}z),
\end{aligned}\tag{2.21}$$

where

$$\nu\equiv l+\tfrac{1}{2},\quad ka\equiv\nu+\nu^{1/3}z,\quad k'a\equiv\nu+\nu^{1/3}z'.\tag{2.22}$$

Ai and Bi are the Airy functions.

Relevant quantities:

$$\begin{aligned}
e^{2i\epsilon_l}&\approx1-i2(6^{1/3})\sin(\tfrac{1}{3}\pi)\frac{\Gamma(\frac{2}{3})}{\Gamma(\frac{1}{3})}z,\\
\Delta_l+iS_l&\approx-ka\binom{6}{\nu}^{1/3}\frac{\Gamma(\frac{2}{3})}{\Gamma(\frac{1}{3})}\left[1+6^{1/3}e^{-\pi i/3}\frac{\Gamma(\frac{2}{3})}{\Gamma(\frac{1}{3})}z\right]e^{-\pi i/3},\\
\beta_l&\approx k'a\binom{6}{\nu}^{1/3}\frac{\Gamma(\frac{2}{3})}{\Gamma(\frac{1}{3})}\left[1-6^{1/3}\frac{\Gamma(\frac{2}{3})}{\Gamma(\frac{1}{3})}z'\right],\\
e^{2i\delta_l}&\approx[(k'+k)\cos\tfrac{1}{6}\pi+i(k'-k)\sin\tfrac{1}{6}\pi]^{-2}\\
&\quad\times\left(k'^2+k^2+kk'-i2(6^{1/3})\frac{\Gamma(\frac{2}{3})}{\Gamma(\frac{1}{3})}\sin\tfrac{1}{3}\pi\right.\\
&\quad\left.\times[(k'^2+k^2)z-kk(z+z')]\right)\\
&\approx1+i\frac{6^{1/6}}{\sqrt{3}}\frac{\Gamma(\frac{2}{3})}{\Gamma(\frac{1}{3})}(k-k')a\nu^{-1/3}\\
&\quad\times[1-(k+k')a\nu^{-1}].
\end{aligned}\tag{2.23}$$

Region D. $l>ka$, $ka\gg1$.

Asymptotic expansions:

$$\begin{aligned}
j_l(ka)&\approx\left(\frac{\pi}{2ka}\right)^{1/2}\frac{e^{\nu(\tanh\alpha-\alpha)}}{(2\pi\nu\tanh\alpha)^{1/2}},\\
n_l(ka)&\approx-\left(\frac{\pi}{2ka}\right)^{1/2}\left(\frac{2}{\pi\nu\tanh\alpha}\right)^{1/2}e^{\nu(\alpha-\tanh\alpha)},\\
j_l'(ka)&\approx\left(\frac{\pi}{2ka}\right)^{1/2}\left(\frac{\sinh2\alpha}{4\pi\nu}\right)^{1/2}e^{\nu(\tanh\alpha-\alpha)},\\
n_l'(ka)&\approx\left(\frac{\pi}{2ka}\right)^{1/2}\left(\frac{\sinh2\alpha}{\pi\nu}\right)^{1/2}e^{\nu(\alpha-\tanh\alpha)},
\end{aligned}\tag{2.24}$$

where

$$\nu\equiv l+\tfrac{1}{2},\quad \nu\,\mathrm{sech}\alpha\equiv ka,\quad \nu\,\mathrm{sech}\alpha'\equiv k'a.\tag{2.25}$$

Relevant quantities:

$$\begin{aligned}
e^{2i\epsilon_l}&\approx1-ie^{-2\nu(\alpha-\tanh\alpha)},\\
\Delta_l+iS_l&\approx-ka(\tfrac{1}{2}\sinh2\alpha\tanh\alpha)^{1/2}e^{2i\epsilon_l},\\
\beta_l&\approx k'a\sinh\alpha',\\
e^{2i\delta_l}&\approx1+i\frac{k\sinh\alpha-k'\sinh\alpha'}{k\sinh\alpha+k'\sinh\alpha'}e^{-2\nu(2-\tanh\alpha)}\\
&\approx1-i\frac{(k^2-k'^2)a^2}{4\nu^2}e^{-2\nu}\left[\ln\frac{2\nu}{ka}-1+\frac{(ka)^2}{2\nu^2}\right].
\end{aligned}\tag{2.26}$$

The factor $e^{2i\delta_l}$ in the partial-wave amplitude α_l has different behavior with respect to the regions defined above. In region A the factor $e^{2i\delta_l}$ depends strongly on the evenness or oddness of the orbital momentum l. We shall manipulate Eq. (2.16) to the form

$$\begin{aligned}e^{2i\delta_l}\approx&\frac{ikk'(\tan k'a+\cot k'a)}{k'^2+k^2+ikk'(\cot k'a-\tan k'a)}e^{-2ika}\\&+(-)^l\frac{k'^2-k^2}{k'^2+k^2+ikk'(\cot k'a-\tan k'a)}e^{-2ika}\\=&\frac{2ikk'e^{-2ika}}{(k^2+k'^2)\sin(2k'a)+2ikk'\cos(2k'a)}\\&+(-)^l\frac{(k'^2-k^2)\sin(2k'a)e^{-2ika}}{(k^2+k'^2)\sin(2k'a)+2ikk'\cos(2k'a)}\\=&T+(-)^lR\quad\text{for}\quad l\ll ka\end{aligned}\tag{2.27}$$

where T and R are just the transmitted and reflected coefficients defined by Eqs. (1.1) and (1.3). From Eqs. (2.11) and (2.14) we observe that the smooth part T in Eq. (2.27) will contribute along with the Fraunhofer term, which is the 1 term in the partial-wave amplitude α_l, to the forward scattering amplitude. By the same token, the nonsmooth part R in Eq. (2.27) gives a contribution to the backward scattering amplitude. In other words, the forward diffraction is associated with the Fraunhofer diffraction and the directed transmission, and the backward diffraction with the directed reflection.

In region B the factor $e^{2i\delta_l}$ does not depend so strongly on the evenness or oddness of the orbital momentum l as in region A. It is this dependence which gives rise to a contribution to the backward scattering amplitude. As far as the backward direction is concerned, the region B should be less important than the region A. In regions C and D the factor $e^{2i\delta_l}$ depends smoothly to the orbital momentum. One should expect a minimal contribution from these regions to the backward amplitude. Nevertheless, the contribution from region B is evaluated in the following by the method of stationary phase.[7] The phase factor $e^{2i\delta_l}$ in Eq. (2.19) is expanded in a power series of Fresnel reflection coefficients from Eq. (2.20):

$$e^{2i\delta_l}\approx e^{-2iA}\sum_{p=0}^{\infty}\epsilon_p e^{2ipA'},\tag{2.28}$$

with the coefficients

$$\begin{aligned}\epsilon_p&=\rho,&&p=0\\&=(1-\rho^2)(-\rho)^{p-1},&&p=1,2,\ldots.\end{aligned}\tag{2.29}$$

Furthermore, the Bessel functions in Eqs. (2.11) and (2.13) are approximated by

$$\begin{aligned}J_0(b\sqrt{-t})\approx&\left(\frac{2}{\pi b\sqrt{-t}}\right)^{1/2}\\&\times\cos[(b\sqrt{-t})-\tfrac{1}{4}\pi]=\left(\frac{1}{2\pi b\sqrt{-t}}\right)^{1/2}\\&\times\sum_{q=-1,1}e^{iq[(b\sqrt{-t})-\frac{1}{4}\pi]+2m\pi(kb-\frac{1}{2})i},\end{aligned}\tag{2.30}$$

$$\begin{aligned}&e^{i(kb-\frac{1}{2})\pi}J_0(b\sqrt{-u})\\&\approx\left(\frac{2}{\pi b\sqrt{-u}}\right)^{1/2}\cos[(b\sqrt{-u})-\tfrac{1}{4}\pi]e^{i(kb-\frac{1}{2})\pi}\\&=\left(\frac{1}{2\pi b\sqrt{-u}}\right)^{1/2}\sum_{q=-1,1}e^{iq[(b\sqrt{-t})-\frac{1}{4}\pi]+i(kb-\frac{1}{2})\pi}\\&\quad\times e^{2m\pi(kb-\frac{1}{2})i}.\end{aligned}\tag{2.31}$$

The added term $2m\pi(kb-\frac{1}{2})$ does not alter the defined Bessel functions where m is any arbitrary integer. Since the differential cross sections near forward direction (2.11) and backward direction (2.14) along with Eqs. (2.30) and (2.31) bear a close similarity, we cast the phase-factor $e^{2i\delta_l}$ contribution from the region B to Eqs. (2.11) and (2.14) in one form:

$$\begin{aligned}F_B\equiv&\frac{1}{2i}\int_B e^{2i\delta_l}e^{ir(kb-\frac{1}{2})\pi}J_0(b\sqrt{-w})bdb\\=&\frac{1}{2i}\left(\frac{1}{2\pi\sqrt{-w}}\right)^{1/2}\sum_{p=0}^{\infty}\sum_{q=-1,1}\int_B\epsilon_p(\sqrt{b})e^{i\xi}db,\end{aligned}\tag{2.32}$$

where

$$\begin{aligned}\xi=&-2A+2pA'+q[(b\sqrt{-t})-\tfrac{1}{4}]\\&+r(kb-\tfrac{1}{2})\pi+2m\pi(kb-\tfrac{1}{2}),\end{aligned}\tag{2.33}$$

$$\begin{aligned}w&=t\quad\text{forward}\\&=u\quad\text{backward},\\r&=0\quad\text{forward}\\&=1\quad\text{backward}.\end{aligned}\tag{2.34}$$

The integral in Eq. (2.32) oscillates. This means that the most contributions to the integral come from the value b_0 where $\mathrm{Re}(\xi)$ is stationary:

$$\begin{aligned}\frac{d}{db}[\mathrm{Re}(\xi)]_{b=b_0}=&q(\sqrt{-w})+2k\beta-2kp\ \mathrm{Re}(\beta')\\&+rk\pi+2m\pi k\,|_{b=b_0}\\=&q(\sqrt{-w})+2k\beta_0-2kp\ \mathrm{Re}(\beta_0')\\&+rk\pi+2m\pi k=0.\end{aligned}\tag{2.35}$$

The quantities β_0 and β_0' are defined by

$$\beta_0=\sec^{-1}(ka/kb_0),\quad\beta_0'=\sec^{-1}(k'a/kb_0).\tag{2.36}$$

[7] See R. G. Newton, *Scattering Theory of Wave and Particles* (McGraw-Hill Book Co., New York, 1966), Applied Mathematics Series 55.

From the method of stationary phase, Eq. (2.32) may be approximately expressed by

$$F_B \approx \frac{1}{2i}\left(\frac{1}{2\pi\sqrt{-w}}\right)^{1/2} \sum_{p=0}^{\infty} \sum_{q=1,-1} \times[\epsilon_p(\sqrt{b})e^{i\xi}]_{b=b_0}\left(\frac{\pi}{|G|}\right)^{1/2} e^{i\frac{1}{4}\pi \operatorname{sgn} G}, \quad (2.37)$$

where

$$G=-\frac{2k}{a}\left[\csc\beta - 2kp \operatorname{Re}\left(\frac{\csc\beta}{k'}\right)\right]_{b=b_0}. \quad (2.38)$$

In order to define Eq. (2.35) one must choose the arbitrary integer m properly. The result (2.37) states that the phase-factor $e^{2i\delta_l}$ contribution to the scattering amplitude from region B is due to the transmission and reflection on the boundary along with internal reflections. The mechanism is similar to that of geometric optics for non-normal incident rays on an optical sphere. These rays will give an important contribution at large scattering angles. In region A the reflection and transmission are due to normal incident rays. The internal reflections from the normal incident rays provide more constructive contribution to the near forward and backward amplitudes than non-normal rays. Thus we conclude, as we did before, that the contribution from region B in the backward direction should be less important than that from region A. The absorption inside the square well damps out the contributions from high-order internal reflections, so we shall retain only lower terms $p=0$, 1 in Eq. (2.37). The incident rays at region B are not normal, and are deflected through some angles. That is to say, the contribution of region B is observed at higher momentum transfer which should satisfy the relation

$$\begin{aligned} &(\sqrt{-t}) \geq \sqrt{2}(b/a)(\operatorname{Re}k'-k) \quad \text{for} \quad p=1, \\ &(\sqrt{-u}) \geq 2\sqrt{2}k[1-(b/a)]^{1/2}, \end{aligned} \quad (2.39)$$

where b_B is the lower boundary for region B. Owing to the absorption of the complex potential, the magnitude of phase factor $e^{2i\delta_l}$ is less than 1, so the Fraunhofer term gives a dominant contribution over the phase-factor term in the forward direction for regions A and B.

In the transition region C, the phase factor in Eq. (2.23) yields a destructive interference with the Fraunhofer term, and depends smoothly on the orbital momentum l. The contribution to the scattering amplitude can be estimated by using the mean-value theorem

$$\begin{aligned} F_C &\equiv \int_C \alpha(b) J_0(b\sqrt{-t}) b\,db \\ &= \frac{1}{2}\frac{6^{1/6}}{\sqrt{3}}\frac{\Gamma(\frac{2}{3})}{\Gamma(\frac{1}{3})}(k-k')a\int_C (kb)^{-1/3} \\ &\quad \times[1-(k+k')a(kb)^{-1}]J_0(b\sqrt{-t})b\,db \\ &\approx \frac{1}{2}\frac{6^{1/6}}{\sqrt{3}}\frac{\Gamma(\frac{2}{3})}{\Gamma(\frac{1}{3})}(k-k')a(k\bar{b})^{-1/3} \\ &\quad \times[1-(k+k')a(k\bar{b})^{-1}] \\ &\quad \times \bar{b}J_0(\bar{b}\sqrt{-t})2k^{-1}(ka)^{1/3}, \end{aligned} \quad (2.40)$$

where $\bar{b}$ is mean value and

$$a-k^{-1}(ka)^{1/3} \leq \bar{b} \leq a+k^{-1}(ka)^{1/3}. \quad (2.41)$$

In the case of the large radius a,

$$F_C \approx 0.213[k'(k'-k)a^2/k^2]J_0(\bar{b}\sqrt{-t}). \quad (2.42)$$

From Eq. (2.42) one can conclude that the region C gives only a contribution in the forward direction; and the order should be comparable to the Fraunhofer diffraction from the A and B regions.

In region D the phase factor $e^{2i\delta_l}$ in Eq. (2.26) yields also a destructive interference with the Fraunhofer term. The partial-wave amplitude in region D involves an exponential damping factor; thus the contribution to the scattering amplitude can be neglected in the case under consideration.

We have tried a naive attempt to fit high-energy elastic scattering data by using the above simple square-well model, with a radius a and a complex momentum k' taken as parameters. By choosing proper parameters, the order of the forward and backward peaks can be produced. However, one has difficulties in accommodating the slope of both peaks. The fact is that the Fraunhofer diffraction is always dominant in the forward direction. The backward peak comes from the reflection of the nearby normal rays which also shows a Fraunhofer-like diffraction peak. In this model, the dependence of momentum k' on the orbital momentum l can be assumed. This is to say that the potential V' in Eq. (2.1) is taken as $V'(l)$. Even in this case, the Fraunhofer diffraction still dominates in the forward direction. However, the fitting in the backward direction can be improved.

Before the end of this section we should comment on the approximation used here. Retaining only the first terms in the asymptotic expansions of the Bessel functions will not be suitable *everywhere* in a given region; in particular, there will be a band between adjacent regions in which more terms should be kept, because of the slow convergence of the expansions. In recent years much attention has been paid to this complicated problem of the slow convergence, and some elegant methods have been developed to handle them. A review and some new developments can be found in the two excellent papers by Nussenzveig,[8] who treats this subject in the case of a real square potential. In such a case there appears the striking phenomenon of the so-called surface waves. These are due to total internal reflections. However, in the complex potential,

[8] H. M. Nussenzveig, J. Math. Phys. **10**, 82 (1969); **10**, 125 (1969); Ann. Phys. (N. Y.) **21**, 344 (1963).

because of the internal absorption, this phenomenon should not be expected. The surface, which is closely related to the orbiting of a particle[9] in classical mechanics, has been considered as a mathematical foundation for describing optical glory. Recently, the surface wave has also been suggested as a model[10] for describing high-energy phenomena, and a best fit has been achieved for π^+p backward scattering. In our proposed model, as we shall see later, the backward scattering is treated as a contribution from the discontinuity on the boundary.

3. DISK-TYPE WELL

It has been shown in Sec. 2 that for a square well, the high-energy process can be treated as that of geometrical optics; in the following we shall adopt this point of view. The optical density of the target particle is described here by the term potential. In the high-energy process, any reasonable theory must take some considerations of the relativistic effect; owing to the Lorentz contraction, the shape of most objects is pancakelike in the relativistic case. Thus, we first consider that it is not appropriate to take an optical object as spherical symmetric. Perhaps it is more adequate to replace the sphere with a disk of thickness d and radius R. The thickness d shall be less than radius R in order to accommodate the Lorentz effect. On the other hand, the uncertainty principle yields a lower limit. With the above consideration in mind, we take

$$d=n\pi/k, \quad n\geq 1. \tag{3.1}$$

The second thing that comes to our attention is that some structures of the particle should also be expressed in the model. It is natural to assume that the particle is denser near the center than away from it. Since we treat the difference $k'-k$ as some complex function of the impact parameter b and momentum k,

$$k'=k+F(b,k), \tag{3.2}$$

where $F(b,k)$ is a monotonic decreasing function of the parameter b. The approach used here is quite closely related to the Serber[11] model. Owing to the particle having finite space extent, the function $F(b,k)$ must satisfy the condition

$$F(b,k)\approx 0 \quad \text{for} \quad b \text{ large}. \tag{3.3}$$

Equation (3.3) will play the role of a cutoff to the high partial-wave amplitudes. So the radius R can be discarded by simply taking $R\to\infty$. The distinction between our model here and the Serber[11] model is the discontinuity in the direction of the relative motion for the scattered particles. As we argued in Sec. 2, the discontinuity is responsible for the backward peak. The rigorous treatment of the postulated model here is tedious. We shall follow the empirical point of view from geometrical optics. The approach here is similar to that of Fernback, Serber, and Taylor.[12] Since we are interested in the scattering amplitude near the forward and backward directions, the rays which denote the partial wave involved are nearly normal to the surface of the disk. The non-normal rays will suffer a large deflection which can only be observed at large scattering angles. These non-normal rays should be excluded from the model. The contribution from the so-called transition region, as region C in Sec. 2, should not be present due to the limit $R\to\infty$. Now the partial-wave amplitude α_l has the form

$$2i\alpha_l\equiv 2i\alpha(b) = \frac{2ikk'e^{-ikd}+(-)^l(k^2-k'^2)\sin(k'd)e^{-ikd}}{(k^2+k'^2)\sin(k'd)+2ikk'\cos(k'd)}-1, \tag{3.4}$$

where k' and k are defined by Eqs. (3.2) and (3.1), respectively.

4. NUMERICAL RESULTS

We now discuss certain properties implied by Eq. (3.4). Since the general behavior of Eq. (3.4) is complicated, we restrict ourselves to a simple case where

$$|F(b,k)|\ll|k| \quad \text{for} \quad \text{all } b. \tag{4.1}$$

The function $F(b,k)$ is defined by Eq. (3.2). From Eq. (4.1) the partial-wave amplitude (3.4) is approximately equal to

$$\begin{aligned}2i\alpha_l\approx{}& e^{iF(b,k)d}-1\\ &+(-)^l(-i)\frac{F(b,k)}{k}\left(1-\frac{1}{2}\frac{F(b,k)}{k}\right)e^{iF(b,k)d}\\ &\times[F(b,k)d\cos(kd)+\sin(kd)]\\ &\equiv f(b)+(-)^l g(b).\end{aligned} \tag{4.2}$$

As has been stated before, the contribution to the forward differential cross section comes mainly from the smooth part $f(b)$, in the odd and even partial-wave amplitudes α_l. That is to say, only the term $f(b)$ will contribute to the forward scattering amplitude. This same term is used in the conventional optical model for describing high-energy scattering in the forward direction. However, in the conventional optical model, it is always assumed that the scattering potential changes very slowly over a distance comparable to the incident wavelength $1/k$. In our model, the potential has a discontinuous jump over a such distance. Nevertheless, the model still gives a forward scattering amplitude like that obtained by the conventional optical model. This seems to imply that the forward scattering amplitude does not depend on the variation of the scattering

[9] K. W. Ford and J. A. Wheeler, Ann. Phys. (N. Y.) **7**, 259 (1959).
[10] H. C. Bryant and N. Jarmie, Ann. Phys. (N. Y.) **47**, 127 (1968).
[11] R. Serber, Phys. Rev. Letters **10**, 357 (1963); Rev. Mod. Phys. **36**, 649 (1964).
[12] S. Fernbach, R. Serber, and T. B. Taylor, Phys. Rev. **75**, 1352 (1949).

potential. On the other hand, the backward scattering amplitude certainly does depend on the variation of the potential. Previous optical models did not worry about this variation of the potential, because they were concerned only with the forward scattering.

Now we wish to exploit the relationship between the forward and backward amplitudes. Let us assume that

$$|F(b,k)d|<1. \tag{4.3}$$

Then the smooth part $f(b)$ of the partial-wave amplitude which contributes to the forward scattering amplitude can be approximated by $iF(b,k)d$. It has been generally assumed that the forward scattering amplitude is purely imaginary. With the above assumption, we can determine the functional form $F(b,k)$ from the high-energy forward elastic scattering data. At high energies the forward differential cross section can be expressed by an exponential function, which indicates that the function $F(b,k)$ has a Gaussian form

$$F(b,k)=ia_1e^{-a_2b^2}, \tag{4.4}$$

where both a_1 and a_2 are functions of the incident momentum k. By a proper choice of the disk width d, the nonsmooth part $g(b)$ of the partial-wave amplitude (4.2) can have the following asymptotic forms for large values of the impact parameter b:

$$g(b)\propto e^{-a_2b^2} \tag{4.5}$$

or

$$g(b)\propto e^{-2a_2b^2}. \tag{4.6}$$

Forms (4.5) and (4.6) indicate that the logarithmic slopes for forward differential cross sections should be the same or twice as large as the backward ones. The high-energy $\pi^- p$ experiments[13] exhibit the latter behavior. Our model gives a relation between the forward and backward differential cross section at a given energy. However, the reported experimental data for forward and backward differential cross sections are obtained at different energies. Here we would like to report the simultaneous fit in both directions for some neighboring incident energies by using the partial-wave amplitude (3.4) and the Gaussian form (4.4). For the 17.0-GeV/c forward and 16.0-GeV/c backward data, we have the fitted parameters[14]

$$\begin{aligned} &kd=19\pi=59.6,\\ &a_1=0.0419\ \text{GeV}/c,\\ &a_2=0.0755\ (\text{GeV}/c)^{-2}. \end{aligned} \tag{4.7}$$

The fitted curves are very similar to the two in Fig. 1. However, in the fitting we used a different parametrization. Our motivation comes from the argument that the inelastic process in the forward direction has been taken care of by the complex wave number k'; however, the inelastic process in the backward direction has not. Let us imagine that there exists some exchange mechanism at the discontinuous boundary. Then, after reflections, some inelastic channels will open, which, in turn, will reduce the scattering amplitude in the backward direction. With the above insight in mind, we replace the partial-wave amplitude (4.2) by

$$2i\alpha_l'\equiv f(b)+(-)^l xg(b), \tag{4.8}$$

where the parameter x is used to describe the inelastic backward process. The introduced parameter x would make the parameter d of the disk width excessive. We shall eliminate the parameter d by simply choosing

$$d=\pi/k. \tag{4.9}$$

These changes [(4.8) and (4.9)] are our new parametrization.

We report four simultaneous fits in both directions for $\pi^- p$ scattering; they are represented, respectively, in Figs. 1–4.

1. 17-GeV/c forward and 16-GeV/c backward data[14]*:*

$$\begin{aligned} &x=0.051,\\ &a_1=0.81\ \text{GeV}/c,\\ &a_2=0.075\ (\text{GeV}/c)^{-2}. \end{aligned}$$

2. 10.8-GeV/c forward and 9.9-GeV/c backward data:

$$\begin{aligned} &x=0.0658,\\ &a_1=0.745\ \text{GeV}/c,\\ &a_2=0.0793\ (\text{GeV}/c)^{-2}. \end{aligned}$$

3. 8.9-GeV/c forward and 8.0-GeV/c backward data:

$$\begin{aligned} &x=0.095,\\ &a_1=0.743\ \text{GeV}/c,\\ &a_2=0.078\ (\text{GeV}/c)^{-2}. \end{aligned}$$

4. 7.0-GeV/c forward and 5.9-GeV/c backward data:

$$\begin{aligned} &x=0.095,\\ &a_1=0.647\ \text{GeV}/c,\\ &a_2=0.084\ (\text{GeV}/c)^{-2}. \end{aligned}$$

In the model there is no spin involved. It is expected that the fitting should be only good for low momentum transfer. The figures show that our model gives satisfactory agreement with the experimental data. Something should be said about the choice of the disk width d. If the width d is taken larger than the one given by Eq. (4.9), then the parameter x will also increase. However, the fitted curves only alter very slightly. The same thing is also true if the parameter x is replaced by the disk width parameter d. In that case the width d

[13] K. J. Foley, S. J. Lindenbaum, W. A. Love, S. Ogaki, J. J. Russell, and L. C. L. Yuan, Phys. Rev. Letters **11**, 425 (1963); E. W. Anderson, E. J. Bleser, H. R. Blieden, G. B. Collins, D. Garelick, J. Menes, F. Turkot, D. Birnbaum, R. M. Edelstein, N. C. Hien, T. J. McMahon, J. Mucci, and J. Russ, *ibid.* **20**, 1529 (1968); A. Ashmore, C. J. S. Damerell, W. R. Frisken, R. Rubinstein, J. Orear, D. P. Owen, F. C. Peterson, A. L. Read, D. G. Ryan, and D. H. White, *ibid.* **21**, 387 (1968); J. Orear, D. P. Owen, F. C. Peterson, A. L. Read, D. G. Ryan, D. H. White, A. Ashmore, C. J. S. Damerell, W. R. Frisken, and R. Rubinstein, *ibid.* **21**, 389 (1968).

[14] We are taking units such that $\hbar=c=1$.

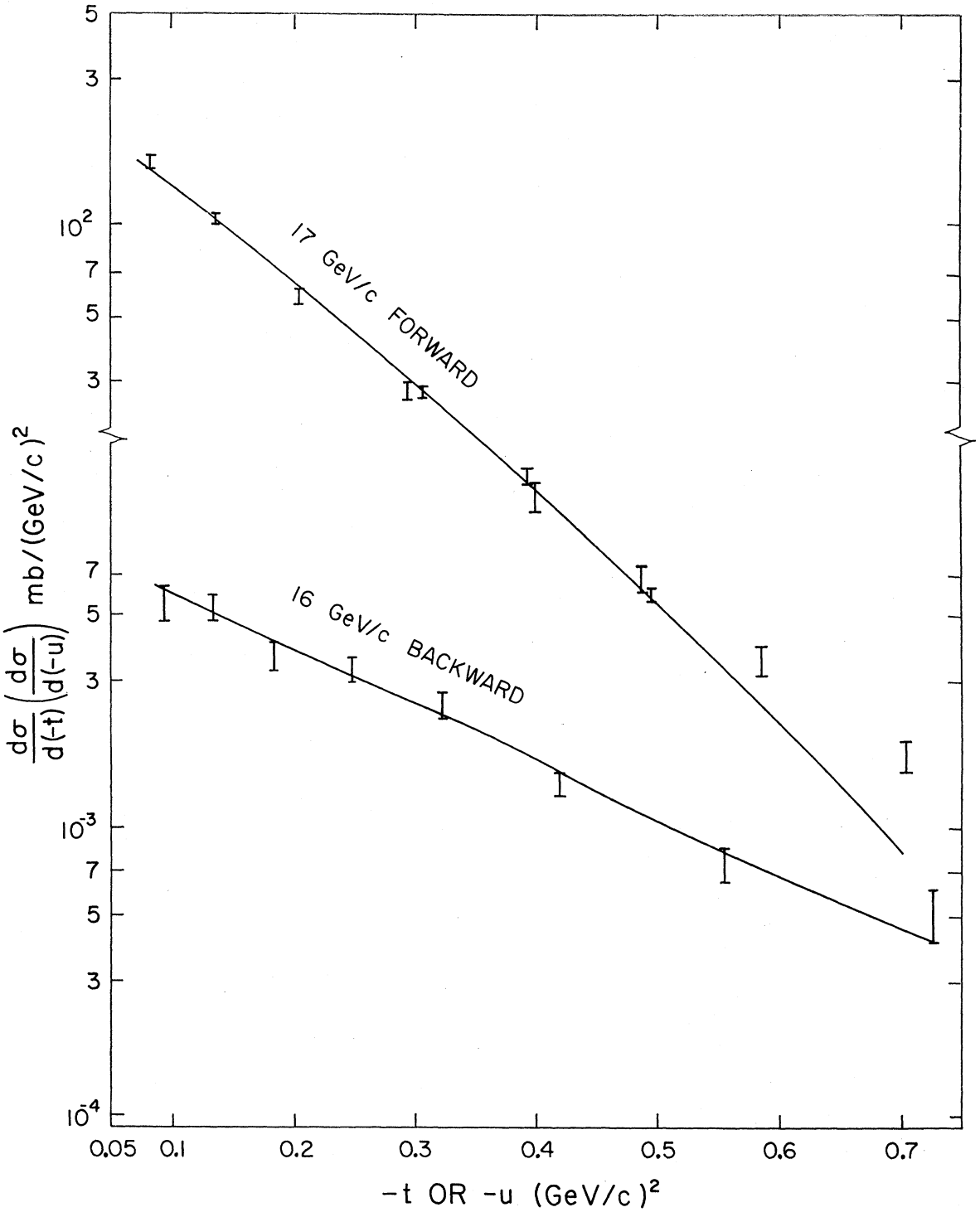

FIG. 1. Simultaneous fit for 17-GeV/c forward and 16-GeV/c backward data in $\pi^- p$ scattering. The three fitted parameters are taken as $x=0.051$, $a_1=0.81$ GeV/c, $a_2=0.075$ (GeV/c)$^{-2}$, where $\hbar=c=1$.

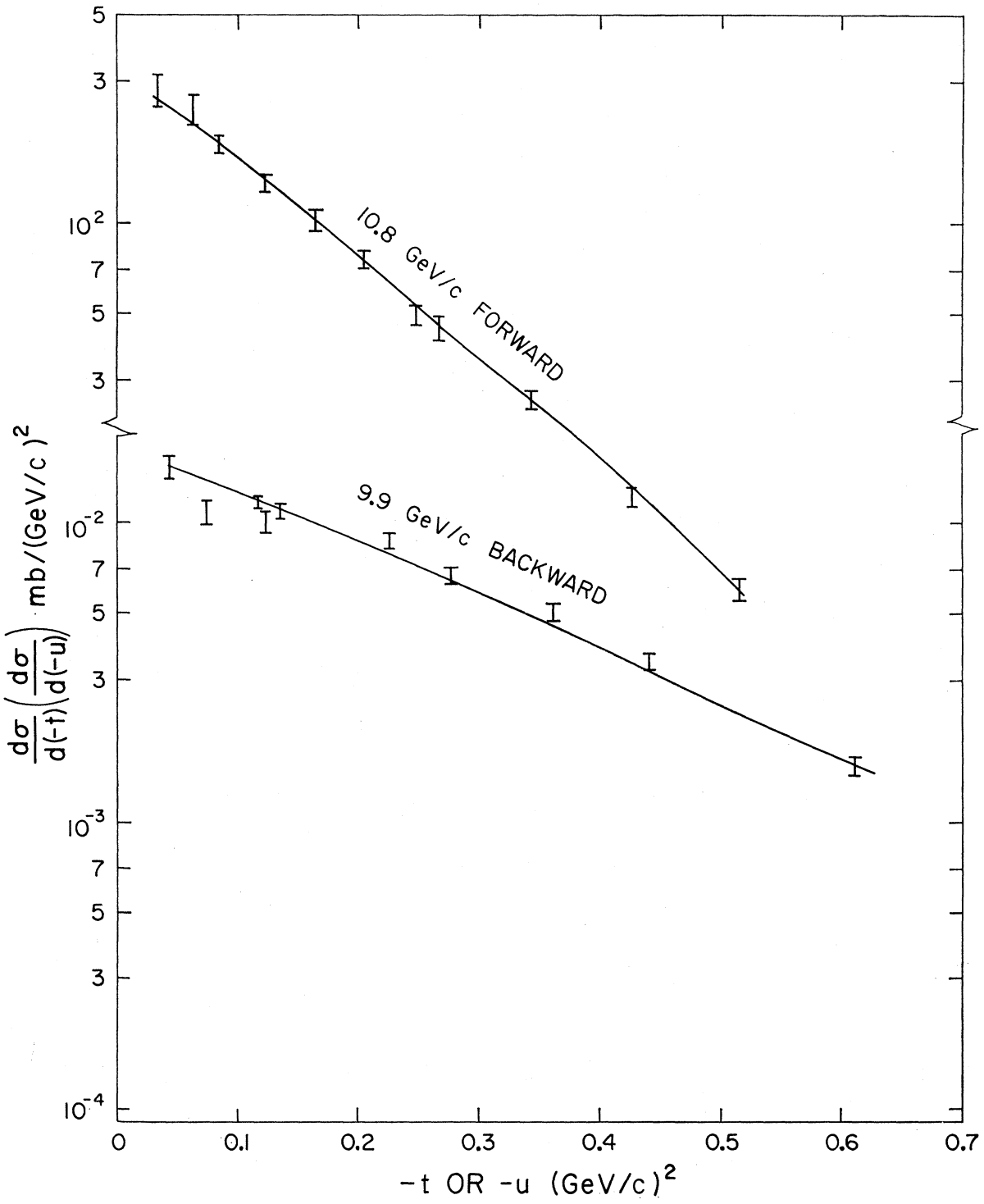

FIG. 2. Simultaneous fit for 10.8-GeV/c forward and 9.9-GeV/c backward data in $\pi^- p$ scattering. The three fitted parameters are taken as $x=0.0658$, $a_1=0.745$ GeV/c, $a_2=0.0793$ (GeV/c)$^{-2}$, where $\hbar=c=1$.

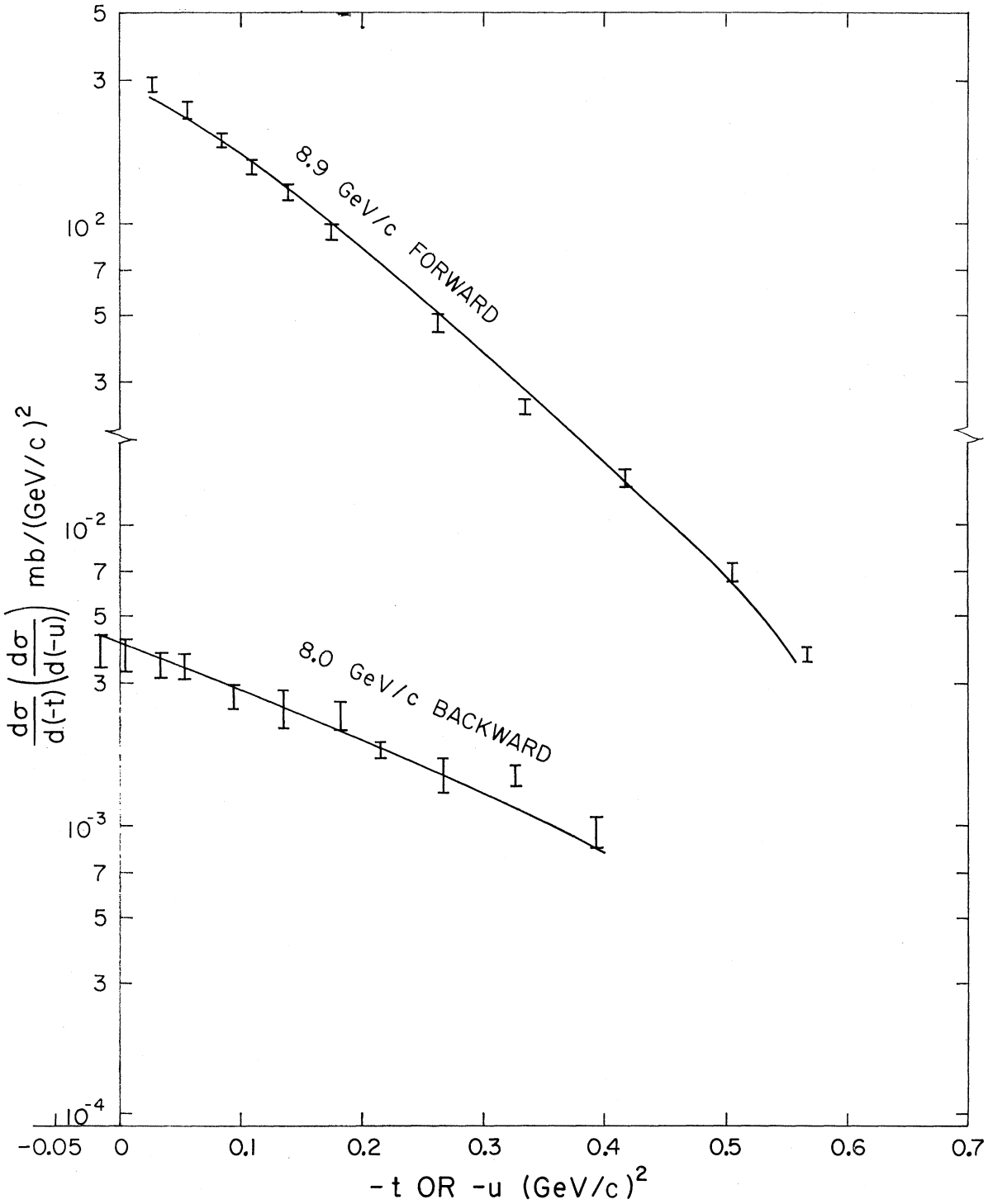

FIG. 3. Simultaneous fit for 8.9-GeV/c forward and 8.0-GeV/c backward data in $\pi^- p$ scattering. The three fitted parameters are taken as $x=0.095$, $a_1=0.743$ GeV/c, $a_2=0.078$ (GeV/c)$^{-2}$, where $\hbar=c=1$.

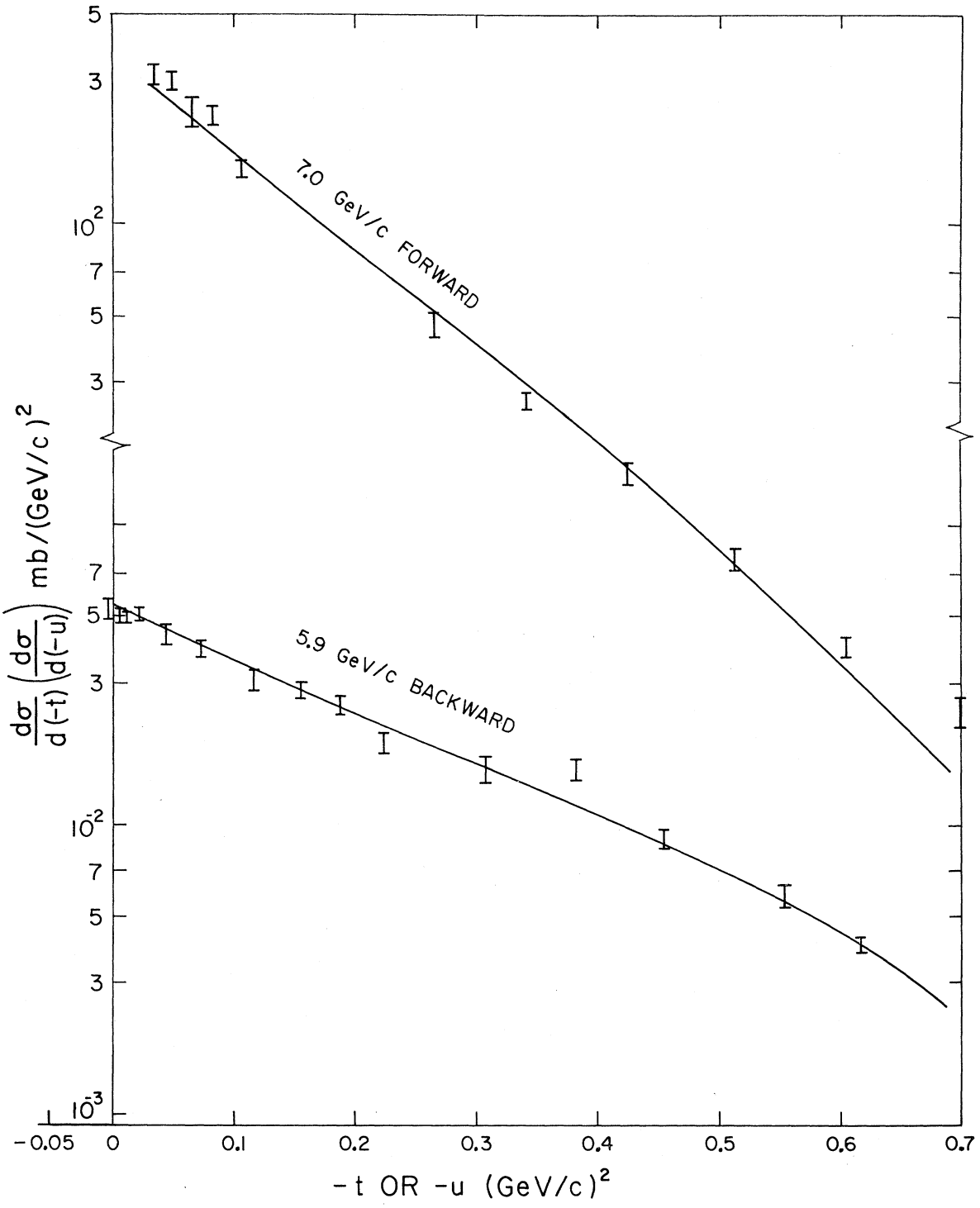

FIG. 4. Simultaneous fit for 7.0-GeV/c forward and 5.9-GeV/c backward data in $\pi^- p$ scattering. The three fitted parameters are taken as $x=0.095$, $a_1=0.647$ GeV/c, $a_2=0.084$ (GeV/c)$^{-2}$, where $\hbar=c=1$.

will vary with the incident energy. All this implies that the goodness of the fit is determined by the model itself and is independent of the choice of the parameter sets. Our choice of parameters is conditioned by the demand that we include the inelastic process in the backward direction. The fitted parameter x decreases as the incident momentum increases. This dependence may reveal the importance of the inelastic process at higher energies. The ratio of the parameter a_1 to the incident momentum k shows a slight decrease as the incident energy increases. This may indicate the transparency of the optical medium at higher energies. The π^+p backward scattering data exhibit more complicated structure than the π^-p data. It is apparent that our simple model cannot accommodate the π^+p backward data. We hope that with some additional mechanism, our simple model may be made to include the π^+p results. The success of the π^-p fits indicates that our model may provide valuable clues as to the nature of high-energy scattering, and that the exchange mechanism is not essential for a description of the backward scattering.

ACKNOWLEDGMENTS

We have enjoyed useful conversations on this subject with our colleagues in the physics department of Virginia Polytechnic Institute. We especially thank Professor R. A. Arndt and Professor S. P. Almeida for helping in the computational programming, and Professor D. Kaplan for reading the manuscript.

PHYSICAL REVIEW D VOLUME 1, NUMBER 1 1 JANUARY 1970

Hadron Couplings in Broken $SU(6)\times O(3)$. I. Baryon Decays

D. L. KATYAL* AND A. N. MITRA
Department of Physics and Astrophysics, University of Delhi, Delhi-7, India
(Received 1 July 1969)

A new form of parametrization is proposed for meson-baryon couplings in a phenomenological quark (Q) model of broken $SU(6)\times O(3)$ for the decays of baryons (mass M) belonging to the representations $(\mathbf{56},2l^+)$ or $[\mathbf{70},(2l+1)^-]$ to baryons (mass m) belonging to $\mathbf{56}$, together with the emission of pseudoscalar (P) mesons (mass μ). The starting point is the use of the direct term in $\bar{Q}QP$ coupling for the evaluation of the meson-baryon coupling structures which are reexpressed in terms of nonrelativistic Rarita-Schwinger fields together with multiple derivative structures in the meson field. A relativistic generalization of the latter is then proposed through a simple extension of the index structures in the $(L+1)$ partial-wave coupling terms. For the $(L-1)$-wave coupling terms, which appear with an extra multiplying factor $\mathbf{k}^2$ in the meson three-momentum $\mathbf{k}$, an additional ansatz $\mathbf{k}^2\rightarrow k_\mu k_\mu$ $(\equiv-\mu^2)$ is used in order to include the contributions of the recoil terms for $(L-1)$-wave transitions in a certain special combination, so as to incorporate the experimental feature of enhanced heavy-meson decays in the s wave. Finally, all these coupling terms are assumed to be multiplied by the following form factor, the plausibility of whose structure is defended on physical grounds: $f_L(k^2)=g_L\mu^{-L-1}(\mu/m_\pi)^{1/2}(\mu/w_k)^{L\pm1}(M/m)^{1/2}$, where the exponents $(L\pm1)$ are used for emissions in the corresponding waves, and g_L is a single free parameter governing the entire supermultiplet transition. The scheme, which is subjected to a detailed experimental test in respect to a large number of baryonic transitions from $(\mathbf{70},1^-)$ and $(\mathbf{56},2^+)$ states involving a wide range of masses and momenta, is found to provide an impressive number and quality of agreements with experiment. It is also shown to yield almost equal values of the coupling constants g_L in respect to the couplings of several Regge recurrences of the Δ resonances, in conformity with the general expectation of a universal coupling for the Regge trajectory of a given particle.

1. INTRODUCTION

ONE of the most fruitful studies of higher resonances has been through their couplings with the **56** baryons and **36** mesons. The usefulness of these couplings lies partly in their mathematical simplicity (being merely three-point functions) and partly in their direct physical manifestations through the two-body decays of various resonances into lighter objects. Moreover, the decay rates of these resonances are generally very sensitive to their spin-parity and $SU(3)$ assignments, so that they provide fairly unambiguous means of testing these assignments without going too much into the details of a theory. In this respect decay properties are a better guide to the identifications of $SU(6)$ quantum numbers for resonances than, e.g., the studies of mass formulas or mass splittings which not only are less sensitive to the input potentials but also are much more model-dependent.

Studies of hadron couplings can be classified under two broad heads, (i) those which are based on fairly elaborate relativistic groups, which leave little scope for parametrization, and (ii) those which use the quark model as a pedagogical device for the evaluation of coupling coefficients in terms of certain phenomenological form factors which are used as free parameters. In the

* Permanent address: Basic Physics Division, National Physical Laboratory, Hillside Road, Delhi-12.